nature astronomy

MATTERS ARISING

https://doi.org/10.1038/s41550-021-01422-z

Check for updates

# No evidence of phosphine in the atmosphere of Venus from independent analyses

**G. L. Villanueva[1]✉, M. Cordiner[1,2], P. G. J. Irwin[3], I. de Pater[4], B. Butler[5], M. Gurwell[6], S. N. Milam[1], C. A. Nixon[1], S. H. Luszcz-Cook[7,8], C. F. Wilson[3], V. Kofman[1,9], G. Liuzzi[1,9], S. Faggi[1,9], T. J. Fauchez[1,10], M. Lippi[1,9], R. Cosentino[1,11], A. E. Thelen[1,10], A. Moullet[12], P. Hartogh[13], E. M. Molter[4], S. Charnley[1], G. N. Arney[1], A. M. Mandell[1], N. Biver[14], A. C. Vandaele[15], K. R. de Kleer[16] and R. Kopparapu[1]**

ARISING FROM J. Greaves et al. *Nature Astronomy* https://doi.org/10.1038/s41550-020-1174-4 (2020)

The detection of phosphine ($PH_3$) in the atmosphere of Venus has been recently reported on the basis of millimetre-wave radio observations[1] and their reanalyses[2,3]. In this Matters Arising we perform an independent reanalysis, identifying several issues in the interpretation of the spectroscopic data. As a result, we determine sensitive upper limits for $PH_3$ in Venus's atmosphere (>75 km, above the cloud decks) that are discrepant with the findings in refs. [1–3].

The measurements target the fundamental first rotational transition of $PH_3$ ($J=1$–0) at 266.944513 GHz, which was observed with the James Clerk Maxwell Telescope (JCMT) in June 2017 and with the Atacama Large Millimeter/submillimeter Array (ALMA) in March 2019. This line's centre is near the $SO_2$ ($J=30_{9,21}$–$31_{8,24}$) transition at 266.943329 GHz (only 1.3 km s$^{-1}$ away from the $PH_3$ line), which represents a potential source of contamination. The JCMT and ALMA data, as presented in ref. [1], are at spectral resolutions comparable to the frequency separation of the two lines. Moreover, the spectral features identified are several kilometres per second in width, and therefore do not permit distinct spectroscopic separation of the candidate spectral lines of $PH_3$ and $SO_2$. We present the radiative transfer modelling we have performed and then discuss the ALMA and JCMT analyses in turn.

## ALMA reanalysis

The analysis of interferometric data is relatively complex, in particular for bright and extended sources such as Venus (15.2 arcsec angular diameter for the ALMA data). The completeness of the different baselines (short and long) determines the ability to accurately measure the total planetary flux density[4], while the bandpass calibration is a crucial factor in the ultimate quality of the resulting spectra[5,6]. The details of the calibration and imaging used during data reduction can have a dramatic impact on the quality and validity of the resulting ALMA interferometric data. The extracted spectra in extended data fig. 4 and the interferometric map in extended data fig. 3 of ref. [1] show large quasiperiodic fluctuations in the spectrum, which in ref. [1] is fitted with high-order polynomials. Particularly challenging is the fact that these fluctuations have a pattern/width comparable to their defined $PH_3$ line core region. As we present in Supplementary Section 2 and as also reported in refs. [7,8], artificially produced features that mimic true atmospheric lines can be produced when analysing data with such characteristics.

Many of these large fluctuations can be introduced by the particular parameters used in calibration during data reduction. After the publication of ref. [1] we notified the North American ALMA Science Center team of substantial differences in the final spectra when applying different treatments of the bandpass calibrations—specifically, the type of bandpass calibration solution (traditional channel to channel versus polynomial fitted versus smoothed), and in particular enabling the 'usescratch=True' setting in Common Astronomy Software Applications (CASA)'s setJy for the model used for Callisto (the bandpass calibrator). The newly reprocessed data from the Joint ALMA Office (JAO) take these issues into consideration and are used by refs. [2,3]. We analysed the data as presented originally in ref. [1] and could not recover a $PH_3$ signature (Fig. 1b), and we also reduced the ALMA data using the new JAO scripts as the starting point. We employed three separate procedures by three different groups (National Aeronautics and Space Administration Goddard Space Flight Center—NASA/GSFC, Berkeley, and National Radio Astronomy Observatory—NRAO), making use of different methods to evaluate the significance of the reported ALMA $PH_3$ signatures. The three methods are the following: (1) employing the updated JAO scripts throughout (using CASA only, done at NASA/GSFC); (2) employing the updated JAO scripts, but proceeding independently beyond self-calibration (using CASA only; done at Berkeley)—note that phase-only self-calibration was done but not amplitude self-calibration, because the latter can be problematic for extended sources[4]; (3) as (2), but with the post-JAO-script reduction done in the Astronomical Image Processing System (AIPS)

[1]Solar System Exploration Division, NASA Goddard Space Flight Center, Greenbelt, MD, USA. [2]Department of Physics, Catholic University of America, Washington, DC, USA. [3]Department of Physics, University of Oxford, Oxford, UK. [4]Department of Astronomy, University of Berkeley, Berkeley, CA, USA. [5]National Radio Astronomy Observatory (NRAO), Socorro, NM, USA. [6]Center for Astrophysics, Harvard & Smithsonian, Cambridge, MA, USA. [7]Department of Astronomy, Columbia University, New York, NY, USA. [8]American Museum of Natural History, New York, NY, USA. [9]Physics Department, American University, Washington, DC, USA. [10]Universities Space Research Association, Columbia, MD, USA. [11]University of Maryland, College Park, MD, USA. [12]SOFIA Science Center, Moffett Field, CA, USA. [13]Max-Planck-Institut fur Sonnensystemforschung, Gottingen, Germany. [14]Observatoire de Paris, LEISA/CNRS, Meudon, France. [15]Royal Belgian Institute for Space Aeronomy, BIRA-IASB, Brussels, Belgium. [16]California Institute of Technology (Caltech), Pasadena, CA, USA. ✉e-mail: geronimo.villanueva@nasa.gov

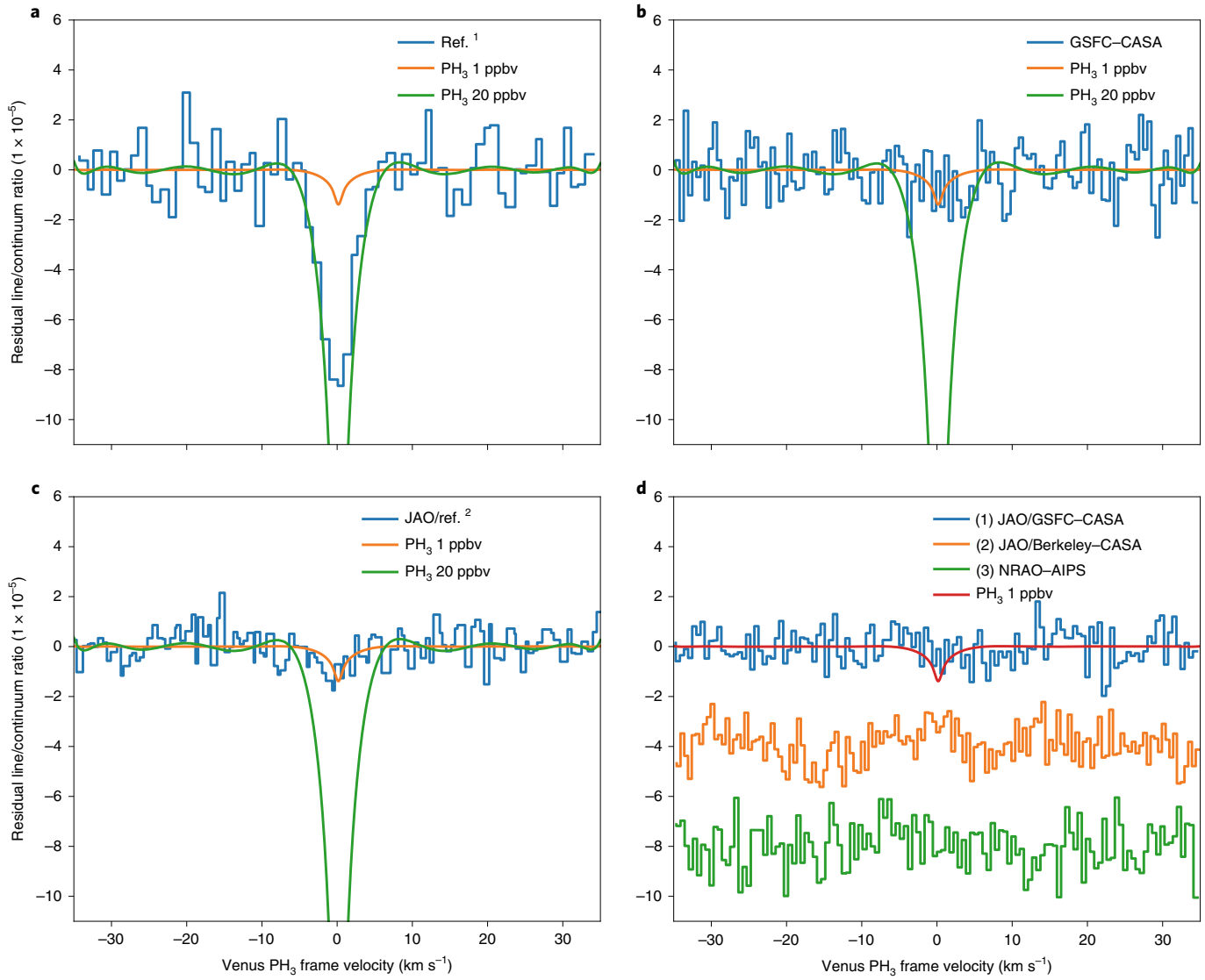


**Fig. 1 | Comparison between the results obtained by the authors of the original paper and its reanalysis and our independent analysis of the same data retrieved from the ALMA science archive. a**, The ALMA data as presented in fig. 2 of ref. [1] for the whole planet (the spectral resolution dv is 1 km s$^{-1}$). **b**, Our original analysis of the raw ALMA data (dv: 0.55 km s$^{-1}$), employing the original ref. [1] scripts but enabling the usescratch=True setting in CASA's setJy, correcting the bandpass calibration. **c**, The reanalysed data presented in ref. [2] using updated scripts; ref. [1] employed a higher (12th-order) polynomial in the bandpass calibration (instead of third order in the JAO script), and excluded short baselines (<33 m) from their analysis (dv: 0.55 km s$^{-1}$). The orange and green lines in **a**–**c** are models of the phosphine line computed with a constant abundance of 1 and 200 ppbv respectively. **d**, Our independent analysis of the JAO-revised ALMA data, employing different methods, a resolution of dv: 0.55 km s$^{-1}$, methods 1 and 2 including all baselines and method 3 excluding <33 m baselines. A sixth-order polynomial was removed for (1) (see details in Methods and in Supplementary Section 2), while only a second was removed for (2) and (3). The red line corresponds to the model with a constant abundance of 1 ppbv $PH_3$.

(using both CASA and AIPS, done at NRAO). We investigated including/removing certain baselines; further details of the methods can be found in Methods and in Supplementary Section 2. All these analyses used the common foundation of the revised JAO scripts to carry out the initial calibration (in particular the bandpass and complex gain versus time calibrations), and very similar steps in the further data reduction (phase-only self-calibration, continuum subtraction, forming the image cube and extracting the disk-averaged spectrum).

The quality of the bandpass calibration was improved with the updated JAO scripts, yet the residual spectrum still showed notable large fluctuations (we found that a sixth-order polynomial captured most of the residual large fluctuations for method 1; ref. [1] considered a 12th order). Our other two reanalyses (2 and 3) led to practically flat spectra only needing second-order polynomial baselines (more information on the origin of these differences is explained in Supplementary Section 2). Ultimately, all our analyses of the data using these different approaches and methodologies reveal no conclusive signature of $PH_3$ (Fig. 1), leading to an upper limit of <1 part per billion by volume (ppbv) ($3\sigma$ when employing a linewidth of 0.186 cm$^{-1}$ atm$^{-1}$. When employing other proposed linewidths, the upper limit would be $PH_3 < 0.7$ ppbv (linewidth of 0.12 cm$^{-1}$ atm$^{-1}$) or <1.5 ppbv (linewidth of 0.286 cm$^{-1}$ atm$^{-1}$). This upper limit is also consistent with other recently reported upper limits derived from infrared ground-based observations ($PH_3 < 5$ ppbv)[9] and from spacecraft data ($PH_3 < 0.2$ ppbv)[10]. We further validated our analysis of the ALMA data by analysing other $SO_2$ and HDO lines in the same dataset (Supplementary Section 3).

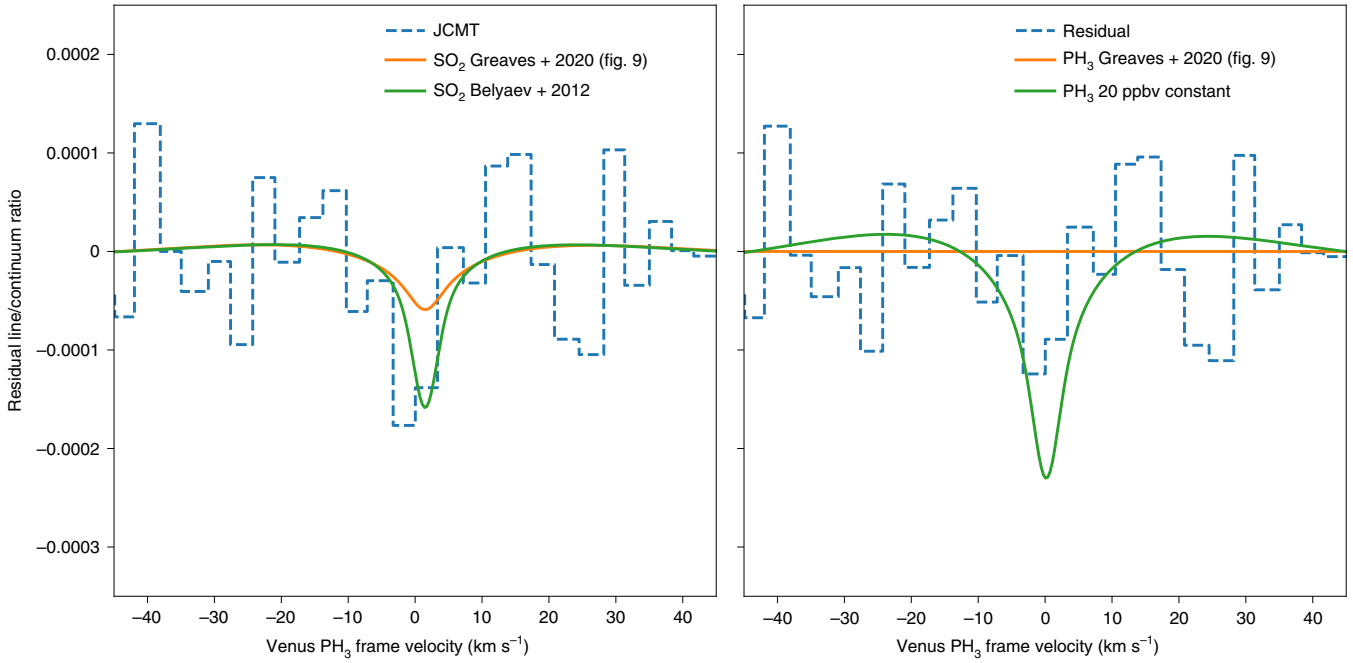


**Fig. 2 | Residual JCMT data and models of $SO_2$ and $PH_3$.** Left: JCMT data for their mid-range solution with masking within ±5 km s$^{-1}$, while '$SO_2$ Greaves + 2020' is a model spectrum synthesized using the *T*–*P* in ref. [1] fig. 8 and the $SO_2$ profile in ref. [1] fig. 9. '$SO_2$ Belyaev + 2012' is a typical profile in ref. [11] (fig. 9) and similar to ref. [12] (case D), with an $SO_2$ abundance of ~30 ppbv at 80 km, increasing to ~100 ppbv at 90 km and reaching ~300 ppbv at 95 km. Right: 'Residual' is obtained by removing the $SO_2$ signature from the JCMT data as modelled with a 3 km s$^{-1}$ resolution using the ref. [1] fig. 9 $SO_2$ profile. The '$PH_3$ Greaves + 2020' spectrum is a model spectrum employing the $PH_3$ profile in ref. [1] fig. 9 (peaking at 60 km with 20 ppbv) and the default linewidth (0.186 cm$^{-1}$ atm$^{-1}$), while a model considering a vertically constant mixing ratio of 20 ppbv is labelled '$PH_3$ 20 ppbv constant'. '$PH_3$ Greaves + 2020' is flat and featureless because these measurements only sample $PH_3$ above 75 km (Supplementary Section 4).

## JCMT analysis and $SO_2$ contamination

The analysis of JCMT spectral data in ref. [1] involved fitting of multiple polynomials for the purpose of continuum subtraction: an initial fourth-order polynomial was removed, then a ninth-order polynomial was removed from a smoothed spectrum and finally a masked eighth-order polynomial was removed. Recently, Thompson[8] explored the robustness of the two detection methods used in ref. [1], namely low-order polynomial fits and higher-order multiple polynomial fits, and found that neither line detection method is able to recover a statistically significant detection at the position of the $PH_3/SO_2$ line.

We investigate whether a weak $PH_3$ signature, if present, could be distinguished from $SO_2$ contamination, and what its contribution to the detected signal could be. To explore this, we employed the same VIRA45 temperature–pressure (*T*–*P*) profile as used by Greaves et al.[1] (their extended data fig. 8) and the $SO_2$ profile presented in their extended data fig. 9 (~100 ppbv in the 70–90 km region, dropping to <30 ppbv above 95 km). If this potential $SO_2$ contaminant signature were removed from the JCMT data, then the original feature would be confined within the noise (Fig. 2). We next modelled a mesospheric $SO_2$ profile as measured by Venus Express using solar occultation[11], and similar to case D of ref. [12] ($SO_2$ abundance of ~30 ppbv at 80 km, increasing to ~100 ppbv at 90 km and reaching ~300 ppbv at 95 km). In this case, the $SO_2$ contamination signature is even stronger and fully captures the claimed $PH_3$ residual in refs. [1–3] (Fig. 2). A comprehensive compilation of $SO_2$ measurements[7,8], including thousands of measurements from the Venus Express orbiter at ultraviolet and infrared wavelengths as well as ground-based observations[11,13–22], show that $SO_2$ abundances at 80 km are frequently well in excess of 100 ppbv, with peak abundances occasionally exceeding 1,000 ppbv. This shows that the $SO_2$ profiles we adopted are well within usual ranges of variability observed on Venus (more information about the considered profiles can be found in Supplementary Section 1). Having shown that the absorption line can be reproduced by a reasonable vertical profile of $SO_2$, we therefore argue that this absorption line cannot be definitively attributed to $PH_3$.

## Probing altitude

We also explored the altitudes from which these absorptions originate, which can be used to constrain photochemical models and facilitate comparison with other measurements[23–27]. This is ultimately related to the spectroscopic parameters of the targeted line and of the competing radiative active species in this spectral region. When considering the linewidth of 0.186 cm$^{-1}$ atm$^{-1}$ for $PH_3$, at 70 km ($3.4 \times 10^{-2}$ atm) the line would be 213 km s$^{-1}$ wide, that is, much broader than the narrow window region of ±5 km s$^{-1}$ or ±10 km s$^{-1}$ searched for $PH_3$. As a polynomial is fitted and subtracted, removing any spectral line information beyond this core region, the spectral information at broader widths (originating from lower altitudes) is thus removed. Our models predict an observable $PH_3$ absorption at this frequency only when $PH_3$ is present above 75 km (see details in Supplementary Section 4), and therefore these data provide no constraints on its abundance in the cloud deck (50–70 km), in contrast to refs. [1–3]. This can be seen in Fig. 2: a flat spectrum is calculated for the $PH_3$ profile determined from the chemical modelling described in ref. [1], in which $PH_3$ is present only below 70 km altitude.

## Conclusions

By our independent analysis of the ALMA data, we set a limit of 1 ppbv for $PH_3$. We also show that the observed JCMT feature could be attributed to mesospheric $SO_2$ gas. Furthermore, for any $PH_3$ signature to be recoverable in either ALMA or JCMT analyses, $PH_3$ needs to be present at altitudes above 75 km. We conclude that the recent identification of $PH_3$ in the upper atmosphere of Venus is not supported.

## Methods

We have employed three independent radiative transfer models: the Planetary Spectrum Generator (PSG; https://psg.gsfc.nasa.gov)[28], the Non-linear Optimal Estimator for Multivariate Spectral Analysis (NEMESIS; https://nemesiscode.github.io)[29] and the Center for Astrophysics planetary modelling tool[30]. The Planetary Spectrum Generator radiative transfer analysis included the latest HITRAN $SO_2$ line parameters for a $CO_2$ atmosphere[31], a layer-by-layer, line-by-line study, and a full disk sampling scheme with 10 concentric rings. The NEMESIS analysis was also performed in line-by-line mode, and used the same spectroscopic data with a five-point Gauss–Lobatto disk integration scheme. As described in ref. [1], there is some uncertainty in the line-shape parameters for the $PH_3$ line in a $CO_2$ atmosphere. HITRAN reports an air linewidth of 0.067 $cm^{-1}$ $atm^{-1}$, which would correspond to 0.12 $cm^{-1}$ $atm^{-1}$ in a $CO_2$ atmosphere if the value were scaled by the typical 1.8 scaling ratio observed for the $SO_2$ lines[32]. Greaves et al.[1] considered a theoretical estimate of 0.186 $cm^{-1}$ $atm^{-1}$, and an upper range of 0.286 $cm^{-1}$ $atm^{-1}$ measured for the $NH_3(J=1–0)$ line in $CO_2$ at 572.498160 GHz. Considering the uncertainty on this parameter, we adopt the same value as Greaves et al.[1] by default (0.186 $cm^{-1}$ $atm^{-1}$).

When reducing the ALMA data, we downloaded the raw data and scripts as provided in the archive. By three separate reduction methods, we then used the provided scripts along with well established techniques in the calibration and imaging of radio interferometric data to obtain final disk-averaged spectra for Venus. There are three scripts provided with the data: (1) a calibration script; (2) an imaging preparation script; (3) an imaging script. The calibration script calculates and applies several system calibrations and flags data known to be invalid, then sets the model for Callisto and uses this for flux density scale and bandpass calibration (using a third-order polynomial fit to the bandpass amplitude), then carries out a complex gain versus time calibration using the calibrator J2000-1748. The imaging preparation script Doppler shifts the spectral axis of the various spectral windows, then images Venus and uses that image to carry out phase-only self-calibration, then sets the model for Venus and carries out amplitude self-calibration.

The imaging script then makes a continuum image, carries out continuum subtraction and makes the image cube. In both the continuum image and the image cube a primary beam correction is made, since the primary beam at these frequencies (with a full-width at half-maximum of ~24″) resolves the disk of Venus (diameter ~15.2″ at the time). We note that the amplitude self-calibration step in the imaging preparation script can lead to problems when observing bright objects with sharp boundaries (such as Venus or Jupiter)[4], and it also leads to the flux density scale being set incorrectly when using these scripts (because it will set the model flux density to that expected for Venus with no primary beam attenuation, but the primary beam actually attenuates that flux density by about 15%, and this attenuation is actually corrected for in the imaging script). All three of our independent analyses used the entire calibration script as provided from the archive. Our first analysis continued with the scripts as provided from the archive throughout, attempting to recreate as closely as possible the analysis in refs. [1–3]. Our second analysis took the data after the Doppler shift step, then proceeded with the reduction within CASA. The only notable difference from the imaging preparation and imaging scripts is the use of a limb-darkened model of Venus for the phase-only self-calibration, and not carrying out amplitude self-calibration at all. Our third analysis was nearly identical to the second, taking the data after the Doppler shift step, but then proceeding within AIPS instead of CASA. The differences in this third analysis were addition of a second bandpass calibration using a model of Callisto, use of the same limb-darkened model of Venus as in the second analysis for the phase-only self-calibration, no use of amplitude self-calibration, and a scaling of the flux densities by the ratio of the expected (primary beam-attenuated) flux density from Venus to that calculated with a fit to the visibilities. Aside from these differences, other steps in our second and third analyses were essentially the same as those in the provided scripts. For the third analysis, baselines with separations less than 33 m were excluded when making the final image cube; for the first analysis, this was investigated and found to reduce the amplitude of the bandpass calibration artifacts, while increasing the (channel-to-channel) spectral noise. No $PH_3$ detection was evident in either case. For all three analyses, we used the entire disk of Venus to create the final spectrum.

## Data availability

This paper makes use of the 2018.A.00023.S ALMA data, available at https://almascience.nrao.edu/asax. The JCMT data are available at https://www.eaobservatory.org/jcmt/science/archive.

Received: 26 October 2020; Accepted: 7 June 2021;
Published online: 16 July 2021

## References

1. Greaves, J. S. et al. Phosphine gas in the cloud decks of Venus. *Nat. Astron.* https://doi.org/10.1038/s41550-020-1174-4 (2020).
2. Greaves, J. S. et al. Reply to: No evidence of phosphine in the atmosphere of Venus from independent analyses. *Nat. Astron.* https://doi.org/10.1038/s41550-021-01424-x (2021).
3. Greaves, J. S. et al. Addendum: Phosphine gas in the cloud decks of Venus. *Nat. Astron.* https://doi.org/10.1038/s41550-021-01423-y (2021).
4. de Pater, I. et al. First ALMA millimeter-wavelength maps of Jupiter, with a multiwavelength study of convection. *Astron. J.* **158**, 139 (2019).
5. Thelen, A. E. et al. Detection of $CH_3C_3N$ in Titan's atmosphere. *Astrophys. J. Lett.* **903**, L22 (2020).
6. Yamaki, H., Kameno, S., Beppu, H., Mizuno, I. & Imai, H. Optimization by smoothed bandpass calibration in radio spectroscopy. *Publ. Astron. Soc. Jpn* **64**, 118 (2012).
7. Snellen, I. A. G., Guzman-Ramirez, L., Hogerheijde, M. R., Hygate, A. P. S. & van der Tak, F. F. S. Re-analysis of the 267-GHz ALMA observations of Venus: no statistically significant detection of phosphine. *Astron. Astrophys.* **644**, L2 (2020).
8. Thompson, M. A. The statistical reliability of 267-GHz JCMT observations of Venus: no significant evidence for phosphine absorption. *Mon. Not. R. Astron. Soc. Lett.* **501**, L18–L22 (2020).
9. Encrenaz, T. et al. A stringent upper limit of the $PH_3$ abundance at the cloud top of Venus. *Astron. Astrophys.* **643**, L5 (2020).
10. Trompet, L. et al. Phosphine in Venus' atmosphere: detection attempts and upper limits above the cloud top assessed from the SOIR/VEx spectra. *Astron. Astrophys.* **645**, L4 (2021).
11. Belyaev, D. A. et al. Vertical profiling of $SO_2$ and SO above Venus' clouds by SPICAV/SOIR solar occultations. *Icarus* **217**, 740–751 (2012).
12. Lincowski, A. P. et al. Claimed detection of $PH_3$ in the clouds of Venus is consistent with mesospheric $SO_2$. Preprint at https://arxiv.org/abs/2101.09837 (2021).
13. Krasnopolsky, V. A. Spatially-resolved high-resolution spectroscopy of Venus 2. Variations of HDO, OCS, and $SO_2$ at the cloud tops. *Icarus* **209**, 314–322 (2010).
14. Sandor, B. J., Todd Clancy, R., Moriarty-Schieven, G. & Mills, F. P. Sulfur chemistry in the Venus mesosphere from $SO_2$ and SO microwave spectra. *Icarus* **208**, 49–60 (2010).
15. Piccialli, A. et al. Mapping the thermal structure and minor species of Venus mesosphere with ALMA submillimeter observations. *Astron. Astrophys.* **606**, A53 (2017).
16. Vandaele, A. C. et al. Sulfur dioxide in the Venus atmosphere: I. Vertical distribution and variability. *Icarus* **295**, 16–33 (2017).
17. Vandaele, A. C. et al. Sulfur dioxide in the Venus atmosphere: II. Spatial and temporal variability. *Icarus* **295**, 1–15 (2017).
18. Vandaele, A. C. Composition and chemistry of the neutral atmosphere of Venus. *Oxford Research Encyclopedia of Planetary Science* https://oxfordre.com/planetaryscience/view/10.1093/acrefore/9780190647926.001.0001/acrefore-9780190647926-e-4 (2020).
19. Encrenaz, T., Moreno, R., Moullet, A., Lellouch, E. & Fouchet, T. Submillimeter mapping of mesospheric minor species on Venus with ALMA. *Planet. Space Sci.* **113–114**, 275–291 (2015).
20. Encrenaz, T. et al. HDO and $SO_2$ thermal mapping on Venus—IV. Statistical analysis of the $SO_2$ plumes. *Astron. Astrophys.* **623**, A70 (2019).
21. Marcq, E. et al. Climatology of $SO_2$ and UV absorber at Venus' cloud top from SPICAV-UV nadir dataset. *Icarus* **335**, 113368 (2020).
22. Encrenaz, T. et al. HDO and $SO_2$ thermal mapping on Venus—V. Evidence for a long-term anti-correlation. *Astron. Astrophys.* **639**, A69 (2020).
23. Mogul, R., Limaye, S. S. & Way, M. Venus' mass spectra show signs of disequilibria in the middle clouds. Preprint at https://doi.org/10.1002/essoar.10504552.1 (2020).
24. Mogul, R., Limaye, S. S., Way, M. J. & Cordova, J. Is phosphine in the mass spectra from Venus' clouds? Preprint at https://arxiv.org/abs/2009.12758 (2020).
25. Seiff, A. et al. Models of the structure of the atmosphere of Venus from the surface to 100 kilometers altitude. *Adv. Space Res.* **5**, 3–58 (1985).
26. Limaye, S. S. et al. Venus atmospheric thermal structure and radiative balance. *Space Sci. Rev.* **214**, 102 (2018).
27. Akins, A. B., Lincowski, A. P., Meadows, V. S. & Steffes, P. G. Complications in the ALMA detection of phosphine at Venus. *Astrophys. J.* **907**, L27 (2021).
28. Villanueva, G. L., Smith, M. D., Protopapa, S., Faggi, S. & Mandell, A. M. Planetary Spectrum Generator: an accurate online radiative transfer suite for atmospheres, comets, small bodies and exoplanets. *J. Quant. Spectrosc. Radiat. Transf.* **217**, 86–104 (2018).
29. Irwin, P. G. J. et al. The NEMESIS planetary atmosphere radiative transfer and retrieval tool. *J. Quant. Spectrosc. Radiat. Transf.* **109**, 1136–1150 (2008).
30. Gurwell, M. A., Bergin, E. A., Melnick, G. J. & Tolls, V. Mars surface and atmospheric temperature during the 2001 global dust storm. *Icarus* **175**, 23–31 (2005).
31. Gordon, I. E. et al. The HITRAN2016 molecular spectroscopic database. *J. Quant. Spectrosc. Radiat. Transf.* **203**, 3–69 (2017).

32. Wilzewski, J. S., Gordon, I. E., Kochanov, R. V., Hill, C. & Rothman, L. S. $H_2$, He, and $CO_2$ line-broadening coefficients, pressure shifts and temperature-dependence exponents for the HITRAN database. Part 1: $SO_2$, $NH_3$, HF, HCl, OCS and $C_2H_2$. *J. Quant. Spectrosc. Radiat. Transf.* **168**, 193–206 (2016).

## Acknowledgements

We would like to commend the team of Greaves et al.[1] for making their data and scripts available. ALMA is a partnership of ESO (representing its member states), NSF (USA) and NINS (Japan), together with NRC (Canada), MOST and ASIAA (Taiwan) and KASI (Republic of Korea), in cooperation with the Republic of Chile. The Joint ALMA Observatory is operated by ESO, AUI/NRAO and NAOJ. The JCMT data were collected under project S16BP007. JCMT is operated by the EAO on behalf of NAOJ, ASIAA, KASI and CAMS as well as the National Key R&D Programme of China (2017YFA0402700). Additional funding support is provided by the STFC and participating universities in the United Kingdom and Canada. We recognize and acknowledge the very significant cultural role and reverence that the summit of Maunakea has always had within the indigenous Hawaiian community. We are most fortunate to have the opportunity to conduct observations from this mountain.

## Author contributions

G.L.V., P.G.J.I., M.G., V.K. and G.L. performed the retrievals and the radiative-transfer modelling. M.C., I.d.P. and B.B. calibrated and analysed the ALMA data. S.N.M., C.A.N., S.H.L.-C., R.C., A.E.T., A.M., E.M.M., S.C., N.B. and K.R.d.K. assisted with the interpretation of the interferometric spectra. C.F.W., S.F., T.J.F., M.L., P.H., G.N.A., A.M.M., A.C.V. and R.K. assisted with the interpretation of the results in the context of the Venusian atmosphere and its photochemistry. All authors contributed to writing and revising the manuscript.

## Competing interests

The authors declare no competing interests.

## Additional information

**Supplementary information** The online version contains supplementary material available at https://doi.org/10.1038/s41550-021-01422-z.

**Correspondence and requests for materials** should be addressed to G.L.V.

**Peer review information** *Nature Astronomy* thanks the anonymous reviewers for their contribution to the peer review of this work.

**Reprints and permissions information** is available at www.nature.com/reprints.

**Publisher's note** Springer Nature remains neutral with regard to jurisdictional claims in published maps and institutional affiliations.